

Published in final edited form as:

Anal Chem. 2009 April 15; 81(8): 2969-2975. doi:10.1021/ac802576q.

# Nanostructure Initiator Mass Spectrometry: Tissue Imaging and Direct Biofluid Analysis

Oscar Yanes<sup>†,‡</sup>, Hin-Koon Woo<sup>†,‡</sup>, Trent R. Northen<sup>†,‡</sup>, Stacey R. Oppenheimer<sup>§</sup>, Leah Shriver<sup>||</sup>, Jon Apon<sup>†,‡</sup>, Mayra N. Estrada<sup>||</sup>, Michael J. Potchoiba<sup>§</sup>, Rick Steenwyk<sup>§</sup>, Marianne Manchester<sup>||</sup>, and Gary Siuzdak<sup>\*,†,‡</sup>

Department of Molecular Biology, Scripps Center for Mass Spectrometry, Department of Cell Biology, The Scripps Research Institute, La Jolla, California 92037, and Department of Pharmacokinetics, Dynamics and Metabolism, Pfizer Global Research and Development, Groton, Connecticut 06340

†Department of Molecular Biology, The Scripps Research Institute.

‡Scripps Center for Mass Spectrometry, The Scripps Research Institute.

§Pfizer Global Research and Development.

\( \text{Department of Cell Biology, The Scripps Research Institute.} \)

#### **Abstract**

Nanostructure initiator mass spectrometry (NIMS) is a recently introduced matrix-free desorption/ionization platform that requires minimal sample preparation. Its application to xenobiotics and endogenous metabolites in tissues is demonstrated, where clozapine and *N*-desmethylclozapine were observed from mouse and rat brain sections. It has also been applied to direct biofluid analysis where ketamine and norketamine were observed from plasma and urine. Detection of xenobiotics from biofluids was made even more effective using a novel NIMS on-surface extraction method taking advantage of the hydrophobic nature of the initiator. Linear response and limit of detection were also evaluated for xenobiotics such as methamphetamine, codeine, alprazolam, and morphine, revealing that NIMS can be used for quantitative analysis. Overall, our results demonstrate the capacity of NIMS to perform sensitive, simple, and rapid analyses from highly complex biological tissues and fluids.

The origins of imaging mass spectrometry (MS) date back to the 1960s when surfaces were analyzed using secondary ion MS (SIMS). More recently, this approach has been extended to biological surface analysis by taking advantage of the softer ionization technologies such as matrix-assisted laser desorption/ionization (MALDI). While these initial studies were largely focused on peptides and proteins (proteomics), there is a growing interest in small molecules (<1500 Da) to examine biological tissues for exogenous and endogenous metabolites (metabolomics). Since it is essential for imaging MS to correlate location with the molecule of interest, spatially defined desorption/ionization sources are used, including: MALDI (laser irradiation), 4,5 SIMS (focused ion beam), 6,7 and, more recently, desorption electrospray ionization (DESI) (gas/liquid spray). Beach approach, however, has unique advantages and limitations: (i) MALDI's sensitivity and spatial resolution are dependent on matrix selection and/or application procedures. The crystallization process is heavily influenced by the presence of salts and surfaceactive compounds, which may disrupt the matrix—analyte cocrystallization process, thereby hindering efficient ion generation. (ii) SIMS has

<sup>\*</sup>To whom correspondence should be addressed. E-mail: E-mail: siuzdak@scripps.edu..

the advantage of being matrix free and has the best spatial resolution ( $\sim$ 100 nm),  $^{11}$  but in contrast to MALDI the ionization often results in extensive fragmentation which complicates characterization. In addition, most commercial SIMS instruments lack tandem MS capabilities, which is critical for metabolite identification.  $^{12}$ ,  $^{13}$  (iii) DESI<sup>8</sup> is a soft ionization and atmospheric pressure technique  $^{14}$  but is currently limited to imaging resolutions (0.25–1 mm) that are lower than MALDI and SIMS. Recently, resolution approaching 40  $\mu$ m was achieved with a typical DESI-MS setup on nonbiological surfaces (i.e., paper and thin-layer chromatography plates).  $^{15}$ 

A new approach, nanostructure initiator mass spectrometry (NIMS), has been recently introduced by Siuzdak and co-workers \$16,17\$ for surface based mass analysis. The NIMS approach is matrixfree and combines high spatial resolution, high sensitivity, soft ionization, and MS/MS capabilities with standard commercial nitrogen or Nd:YAG (frequency-tripled) laser-source instruments. NIMS utilizes "initiator" molecules trapped in nanostructured surfaces or "clathrates" to release/ionize intact molecules adsorbed from the surface.

An extension of NIMS tissue imaging is the direct analysis of biofluids. <sup>18</sup> Mass profiling of human biofluids has been used for the identification of disease-associated endogenous metabolite biomarkers as well as high-throughput clinical assays (i.e., neonatal screens). <sup>19</sup> As spatially defined desorption/ionization sources are not necessary, these are conventionally performed using GC/MS, LC/ESI-MS, <sup>18</sup> and to a lesser degree MALDI MS. <sup>20</sup> All of which are limited by requisite sample pretreatment (e.g., fractionation, desalting) <sup>21,22</sup> to minimize ion suppression. Recently, DESI MS has been also applied for metabolite analysis in biofluids <sup>23</sup> with minimal sample preparation.

Here we demonstrate the potential of NIMS for clinical applications to tissue imaging MS and direct analysis of biofluids. The potential of NIMS for clinical analytical research is demonstrated with the detection and localization of xenobiotics such as clozapine and *N*-desmethylclozapine in brain tissues. Nicotine, ketamine, and their metabolites (cotinine and norketamine, respectively) together with diazepam and raclopride were detected from biofluids such as saliva, urine, and blood with minimal sample preparation. The performance of NIMS for quantitative goals has been also evaluated with different xenobiotics.

#### EXPERIMENTAL SECTION

#### **Materials**

Hydrofluoric acid (HF), ethanol, acetone, formic acid, acetonitrile (ACN), and methanol were purchased from Fisher Scientific (Fair Lawn, NJ) at the highest purity available. BisF17 was purchased from Gelest (Tullytown, PA). Single side polished P/Boron-type,  $\langle 100 \rangle$  orientation, low resistivity (0.01–0.02  $\Omega$  cm), 525  $\pm$  25  $\mu$ m thick and 100 mm of diameter silicon wafers were obtained from Silicon Valley Microelectronics, Inc. (Santa Clara, CA).  $\alpha$ -Cyano-4-hydroxycinnamic acid ( $\alpha$ -CHCA), clozapine, ketamine, diazepam, raclopride, aprazolam, codeine, methamphetamine, morphine, and morphine- $d_3$  were from Sigma-Aldrich (St. Louis, MO).

#### Instrumentation

An etching chamber was constructed in house, and power was generated from a BIO-RAD PowerPack1000 (Hercules, CA) (see details at

http://masspec.scripps.edu/research/nims/create.php). Laser-NIMS and MALDI were performed using an VoyagerDE STR (Applied Biosystems Inc., Foster City, CA), equipped with delayed extraction (DE) and a 337 nm pulsed nitrogen laser. Digital images are acquired through a Retiga EXi Fast 1394 Mono Cooled digital camera (Qimaging, Burnaby, BC,

Canada). Images of the tissue slice on the NIMS surface were acquired with a microscope Arcturus PixCell II Laser Capture Microdissection (LCM). This instrument is attached to an Olympus IX 50 and is equipped with a Hitachi CCD color camera (KP-D580).

## **NIMS Chips Preparation**

Low resistivity (0.01–0.02  $\Omega$  cm) P-type  $\langle 100 \rangle$  (Boron) silicon was etched with 48 mA/cm<sup>2</sup> (300 mA for the 2.5 cm  $\times$  2.5 cm etching cell used in this work) for 30 min. Neat initiator (BisF17) solution was applied at room temperature for 30–60 min to the surface and excess initiator was removed using a jet of nitrogen. Please refer to Woo et al. <sup>17</sup> and http://masspec.scripps.edu/research/nims/create.php for additional details on the step-by-step preparation of NIMS surfaces.

## **Adult Rat and Mice Tissue Slices Preparation**

Adult male mice (Balb/cByJ) were obtained from the Scripps Research Institute Rodent Breeding Colony and used according to Institutional Animal Care and Use Committee (IACUC) approved protocols. Mice and rat were deeply anesthetized by isofluorane inhalation and sacrificed by cervical dislocation. Organs were collected, quickly frozen in Optimum Cutting Temperature (OCT) compound embedding medium (VWR International, West Chester, PA) on dry ice, equilibrated to -20 °C, sectioned at 3–5  $\mu$ m, and collected on the NIMS surface. Representative sections were collected on Superfrost Plus slides (Fisher Scientific, Pittsburgh, PA) and stained with hematoxylin and eosin using routine histological techniques. All procedures involving mice and rats were approved by the Institutional Animal Care and Use Committee at The Scripps Research Institute (TSRI) and conform to National Institutes of Health guidelines and public.

## Laser-NIMS and MALDI

Mass spectra of biofluids were performed on a Voyager-DE STR mass spectrometer (Applied Biosystems Inc., Foster City, CA) with delayed extraction (DE) and a 337 nm nitrogen laser. Bradykinin fragment 1-8 (904.0273 m/z) and acetylcholine (146.1181 m/z) were used for external calibration. Each recorded mass spectrum is the result of analyzing 500 laser shots on the area of interest. Acquisition parameters were set as follows: m/z 100-2000, acceleration voltage 20 kV, grid voltage 60%, mirror voltage ratio 1.12, guide-wire voltage 0.2%, and extraction delay time 100 ns.

#### **Ketamine Administration**

Mice were injected intravenously in the tail vein, using either 0.25 mg/animal ketamine (ketaset, Fort Dodge Animal Health, Fort Dodge IA) diluted in 100  $\mu$ L of PBS or 100  $\mu$ L of a PBS-only control. Animals were sacrificed at either 5, 30, 60, or 120 min postdosing. For each of the time points, kidney, liver, brain, heart, calf muscle, blood, and urine were collected. Blood (serum) and urine were stored at -80 °C. Organs and tissues were embedded in OCT medium (Tissue-Tek, Inc., Sakura Finetek U.S.A, Torrance, CA) in cryomolds and stored at -20 °C.

# **Clozapine Administration**

For the 3–12 mg/kg dose, mice were injected intravenously in the tail vein using either 3, 6, or 12 mg/kg of clozapine diluted in  $200\,\mu\text{L}$  of 0.9% sterile sodium chloride with the pH adjusted to 5 using acetic acid. Animals were sacrificed at 60 min postdosing and intracardially perfused with PBS. Tissues were frozen in OCT medium (Tissue-Tek, Inc., Sakura Finetek U.S.A, Torrance, CA) in cryomolds and stored at  $-80\,^{\circ}\text{C}$  until cryosectioning.

For the 100 mg/kg dose, one 7 week old male Long-Evans rat weighing 234 g was acclimated to standardized housing and feeding conditions in accordance to Animal Care and Use Procedures established at Pfizer which were in agreement with National Institutes of Health guidelines. Feed and water were provided *ad libitum*. Clozapine was administered subcutaneously (100 mg/kg) in a solution of 0.1 N HCl. This clozapine dosed rat was euthanized by  $\rm CO_2$  asphyxiation at 60 min postdosing. The brain was then removed, wrapped in aluminum foil, and frozen by immersion in liquid nitrogen. The sample was stored at  $\rm -20~^{\circ}C$  until cryosectioning.

## **Tissue Imaging**

The 100 mg/kg and 6 mg/kg clozapine dosed brain were sectioned (5 and 3  $\mu$ m thick, respectively, sagittal) on a Leica CM3050 cryostat (Leica Microsystems Inc., Germany), thawmounted onto the NIMS chip, and stored at ambient conditions for ~30 min prior to mass spectrometry analysis. Image acquisition was performed on an Autoflex III MALDI TOF/TOF mass spectrometer (Bruker Daltonics) (100 mg/kg dose) or on a 4700 Proteome Analyzer MALDI-TOF/TOF mass spectrometer (Applied Biosystems) (6 mg/kg dose) in positive, reflector MS mode with the laser operating at 10 (50 laser shots per spot) or 200 Hz (1000 laser shots per spot), respectively. The image was acquired with FlexImaging (Bruker Daltonics) or oMALDI softwares, respectively, at a resolution of 100  $\mu$ m × 100  $\mu$ m, and data viewing and image reconstruction was performed in BioMap software.

## **Direct Analysis of Biofluids**

Fresh human saliva and urine and mouse urine and blood samples were spotted directly onto the NIMS surface without any further sample preparation. After 30 s, urine, blood, and saliva drops were blown-off with a nitrogen stream.

## NIMS in Situ Organic Solvent Extraction

After deposition of  $1-2 \mu L$  of biofluid on the NIMS surface for 30–60 s, the excess is removed by pipetting it out. Methanol extraction is performed by touching the surface (by pipeting it in and out the pipet tip 10–20 times) with 1–2  $\mu L$  of 20% methanol/water, to further deposit it onto an adjacent spot. The original spot is washed out 3 more times with 20% methanol/water following the same protocol and the solution is discarded. Extraction from the original spot with 50%, 80%, and 100% methanol/water is performed in the same way.

#### **Metabolite Identification**

Putative metabolites were identified based on postsource decay (PSD) fragment ions and exact mass (*m*/*z*) using METLIN (http://metlin.scripps.edu/), Human Metabolome Project (http://redpoll.pharmacy.ualberta.ca/hmdb/ HMDB/), and Lipid Maps (http://www.lipidmaps.org/) databases.

# **RESULTS AND DISCUSSION**

## Detection of Clozapine and N-Desmethylclozapine in Brain Tissue

Tissue imaging using MALDI with tandem mass spectrometry (MS/MS) has been used for the analysis of drugs and their metabolites, <sup>24</sup> in which the molecular ion of the analyte is fragmented, and images are generated from one or more analyte-specific fragment ions. However, this approach cannot circumvent signal suppression effects of the matrix (i.e., matrix suppression effects)<sup>25</sup> where the interference from abundant matrix-related ions compromises its ability to ionize intact small molecules in tissues.

NIMS tissue imaging is accomplished by placing cryo-sliced tissues directly on the NIMS surface followed by NIMS analysis. During the early stages of NIMS development,  $^{16}$  an initial ablation step (high laser energy) was applied to remove the surface layer of the tissue ( $\sim$ 12  $\mu$ m thick sections) followed by the acquisition of the mass spectra (low laser energy) at the NIMS tissue/surface interface, where it is believed the metabolites become locally adsorbed to the NIMS surface. This approach has been improved by placing cryo-sliced tissues of 2–4  $\mu$ m thickness on the NIMS surface (Figure 1A). This allows ablation and acquisition to take place simultaneously at the same laser energy ( $\sim$ 0.1 J/(cm² pulse)), facilitating direct tissue analysis using commercially available MS imaging software (e.g., flexImaging, oMALDI).

The spatial resolution of NIMS is essentially limited by the focused width of the laser spot. In our current instrument (VoyagerDE STR), the focused laser beam diameter is approximately  $10-15 \,\mu\text{m}$ , which produces ablated areas of  $15-20 \,\mu\text{m}$  as revealed by the photograph captured by microscope of the tissue slice after five laser pulses (Figure 1B).

The NIMS imaging approach was applied to rat brain tissue dosed 1 h prior with 100 mg/kg of clozapine, in full-scan MS mode (m/z 100-1000). Intact clozapine was observed with no fragmentation and no background interference (Figure 1A). The characteristic chlorine isotopic distribution was observed for clozapine (Figure 1A, inset). NIMS postsource decay (PSD) of clozapine was also employed to confirm the identity of the protonated drug (data not shown). In contrast to NIMS, MALDI analysis of the same sample using the  $\alpha$ -CHCA matrix results in lower sensitivity and extensive fragmentation of clozapine (predominant fragment ion at m/z 270, with other fragment ions observed at m/z 227 and 192, data not shown). N-Desmethylclozapine (m/z 313.11), one of the major clozapine biologically active metabolites, was also detected within the same full-scan analysis of the rat brain. The metabolite generated NIMS spectra with lower signal intensity than clozapine (Figure 1A inset), although localization correlated well with the drug (Figure 1C). Control brain tissue (no clozapine dose) was also performed in full-scan MS mode with no detectable peaks corresponding to clozapine (m/z 327.13) nor its N-desmethylclozapine metabolite (m/z 313.11) (data not shown).

The localization of clozapine in brain tissues by NIMS is consistent with previous MALDI<sup>26</sup> and DESI<sup>27</sup> imaging MS results. The NIMS brain image displays clozapine (Figure 1C) mainly localized in the hippocampus (limbic system). Clozapine is classified as an atypical antipsychotic drug because its profile of binding to serotonergic as well as dopamine receptors. In particular, clozapine interferes to a lower extent with the binding of dopamine at D1, D2, D3, and D5 receptors and has a high affinity for the D4 receptor. Localization of clozapine found here is consistent with its affinity binding to dopamine receptors and indicates that clozapine is preferentially more active at limbic than at striatal dopamine receptors.

NIMS also provides the advantage of allowing higher sensitivity. The sensitivity limit (signal-to-noise >20) for clozapine was established at a 3 mg/kg dose, which exceeds any previous reported measurement of this drug in brain tissue by MALDI MS<sup>26</sup> or DESI MS.<sup>27</sup> This is of particular importance because such concentrations are consistent with dosages used in human studies.<sup>29</sup> At 6 mg/kg dose (Figure 1C), the clozapine molecular ion appears to be exclusively located in the lateral ventricle, in agreement with previous results<sup>30</sup> of clozapine by MALDI MS/ MS as well as autoradiography.<sup>26</sup> It is worth noting that, at this low dose, the intensity of *N*-desmethylclozapine ion was not sufficient to reconstruct an image of the drug metabolite. Importantly, animal dosing in Hsieh et al.<sup>26</sup> for MALDI analysis was 5 mg/kg administered directly into the rat brain, whereas our limit for clozapine was reached at 3 mg/kg administered intravenously in the tail vein. Wiseman et al.<sup>27</sup> dosed animals at 50 mg/kg via oral gavage for DESI analysis. In addition, both previous approaches have used tandem mass spectrometry (a quadrupole-time-of-flight and a linear ion trap, respectively) in order to increase chemical specificity, whereas in the absence of interfering matrix peaks we have used full-scan MS

mode. In fact, Wiseman et al.<sup>27</sup> also imaged the tissue in full-scan MS mode, but the signal-to-noise, in the absence of the chemical specificity of tandem mass spectrometry (MS/MS), was not sufficient to reconstruct an image of clozapine as stated by the authors.

We postulate that NIMS sensitivity could be increased when coupled to MS/MS instrumentation. However, the MS-only mode gives more advantages in that many metabolites are detected at the same time from the same tissue spot, allowing one in principle to simultaneously measure alterations of an administered therapeutic agent and the resulting endogenous molecular changes in tissues. This is clearly the main advantage of a MS platform among autoradiography, the gold-standard method for drug distribution studies. Although sensitivity of radiolabeled isotopes can be higher than NIMS imaging, autoradiography can only visualize total labeled-related compounds, lacking the molecular specificity obtained by mass spectrometry. In addition, the availability of radiolabeled compounds at the drug discovery stage is often limited.

## **Direct Analysis of Xenobiotics in Biofluids**

Much like tissues, the nature and complexity of biofluid samples  $^{18,31}$  typically require sample preparation prior to mass spectrometry analysis, i.e. organic solvent extraction and separation by liquid chromatography. NIMS also allows for the analysis of biofluids without any sample preparation. Two sample deposition methods were developed allowing for the adsorption onto the hydrophobic perfluorinated surface: (i)  $1-2\,\mu\text{L}$  of biological sample in solution can be deposited on the surface and blown off with a stream of nitrogen after  $30-60\,\text{s}$  or (ii) the sample is directly deposited by "Z-touch",  $^{32}$  in which the sample is allowed to sit on the surface before being pipetted off, leaving behind adsorbed metabolites. The rationale behind these deposition methods is to minimize deposited sample thickness, which can ultimately shield the NIMS fluorinated surface from the laser.  $^{17}$  When this occurs, sample can also be removed via laser ablation or, because of the high sensitivity of NIMS, sample dilution has proven to be very effective at improving signal intensity.

NIMS analysis (full-MS mode) of ketamine in plasma and urine from anesthetized mice 5, 30, and 120 min after administration is shown in Figure 2. Although ketamine is known to be rapidly cleared from the system,  $^{33}$  ketamine signal (m/z 238.09) was detected in urine 120 min after administration. The relative intensity of ketamine in plasma is lower than in urine, probably due to rapid clearance from blood and the extremely complex nature of blood where the endogenous metabolites may suppress the ketamine signal. Norketamine (m/z 224.08), a metabolite of ketamine, is also detected in plasma and urine. Similar relative intensities of ketamine and norketamine in plasma at the 30 min time point is observed, consistent with previous studies.  $^{33}$ 

Some xenobiotic compounds can be difficult to detect in complex biological matrixes due to their low concentrations, their intrinsic variable ionization, and the highly variable composition of the matrix. The physicochemical properties of the perfluorinated initiator (BisF17) used in NIMS partially circumvents signal suppression due to these issues because it not only enhances laser desorption of biomolecules, but it also performs as a reverse-phase material due to its high hydrophobicity. In a similar manner to liquid chromatography, compounds can be selectively eluted (in this case extracted) from the surface by extraction with increasingly higher percentages of organic solvents. This was demonstrated on human saliva (Figure 3A), which shows direct analysis of a nonsmoker's saliva by NIMS and the extracted molecules at 20%, 50%, 80%, and 100% methanol/water. The number of different m/z values observed becomes ~10 times greater by using this extraction method. It should also be noted that at higher methanol content the phospholipid signal intensity improves, likely due to the presence of salivary cells (e.g., mucous epithelial cells, blood morphotic elements) as these metabolites are important building blocks of most cellular membranes. The peak detected at m/z 104.11 in

the direct analysis of saliva is associated with choline, which is present in saliva at >10  $\mu$ mol/L. Also, other common LC solvents have been successfully used for extraction (e.g., acetonitrile and ethanol with and without 0.1% trifluoroacetic or formic acid), increasing the number of observed molecules (data not shown). On-chip fractionation of exogenous small molecules such as nicotine from saliva and diazepam and raclopride (50–100 ng/mL) from urine samples were also examined. NIMS mass analysis (Figure 3B) generated a signal consistent with nicotine after *in situ* extraction with 20% methanol of a smoker's saliva. Cotinine, a major metabolite of nicotine, is also detected in saliva (Figure 3B, inset). Diazepam and raclopride were extracted from the chip with 80% methanol. It is worth noting that nicotine can be observed directly (no on-plate extraction) from saliva albeit lower intensity, whereas diazepam and raclopride were not detectable directly from urine at the concentration assayed. It is also important to highlight that sample deposition, *in situ* organic solvent extraction, and analysis could all be performed in less than 10 min for each drug and are easily automatable.

Several standard xenobiotics spiked into rat serum were used to evaluate NIMS performance. Table 1 shows the limit of detection (LOD) for the pure compounds (methamphetamine, codeine, apralozam, and morphine) and the range of linear response in serum. All the compounds show LOD values in the attomole range and very similar linear response when spiked in serum, ranging between 1 and 150 ng/mL (Figure 4). Although NIMS has a high tolerance for salts and other contaminants as demonstrated in Figure 2, NIMS performance is reduced at high sample concentrations. For example, the signal intensity plateau  $^{17}$  for most of the compounds tested above  $^{\sim}200$  ng/mL is probably due to coating thickness of the sample shielding the NIMS surface from the laser. A deuterated form of morphine was used as an internal standard in serum to evaluate the accuracy of NIMS for absolute quantitation (Figure 4D). Morphine was spiked in serum at 10, 50, 150, 250, and 500 ng/mL with morphine- $d_3$  at 100 ng/mL. Above 1000 ng/mL, the NIMS signal intensity plateaued. Overall, these NIMS results show its capability for drug quantitation directly from biological samples with minimal sample preparation.  $^{17}$ 

#### CONCLUSION

NIMS is a soft matrix-free desorption/ionization approach for tissue and biofluid analysis of xenobiotics and endogenous metabolites. NIMS can efficiently desorb and ionize molecules directly from highly complex tissue and liquid matrixes (i.e., saliva, blood) containing cells, salts, and a huge diversity of biomolecules (e.g., proteins, lipids, sugars, etc). In addition, the perfluorinated siloxane compound performs as a reverse-phase-like material by forming a liquid fluorous phase into which analyte molecules become adsorbed. In contrast to MALDI, sensitivity of NIMS ionization is not compromised in the low m/z region due to matrix ion interferences. Coupling NIMS to other surface analysis instrumentation with MS/MS capabilities (i.e., CID in TOF—TOF instruments) or high mass accuracy analyzers such as Fourier transform mass spectrometry (FTMS) will further enable metabolite characterization. Also, further evaluation of NIMS coupled to analyzers that increase specificity (e.g., quadrupole-time-of-flight or linear ion trap) will likely increase sensitivity. It is also possible that new initiators and/or novel nanostructured surfaces will enhance desorption/ionization and broaden the applicability of NIMS.

## **ACKNOWLEDGMENT**

Financial support was received from the Department of Energy (Grants FG02-07ER64325 and DE-AC0205CH11231) and the National Institutes of Health (Grants 5P30MH062261-08 and R24 EY017540). We thank Ole N. Jensen and Anders Nordström for comments.

# References

- (1). Morabito J. Anal. Chem 1974;46:189-196.
- (2). Cornett DS, Reyzer ML, Chaurand P, Caprioli RM. Nat. Methods 2007;4:828–833. [PubMed: 17901873]
- (3). Liu Q, Xiao Y, Pagan-Miranda C, Chiu YM, He L. J. Am. Soc. Mass Spectrom 2008;20:80–88. [PubMed: 18926722]
- (4). Caldwell RL, Caprioli RM. Mol. Cell. Proteomics 2005;4:394–401. [PubMed: 15677390]
- (5). Chaurand P, Stoeckli M, Caprioli RM. Anal. Chem 1999;71:5263–5270. [PubMed: 10596208]
- (6). Burns-Bellhorn MS, File DM. Anal. Biochem 1979;92:213–221. [PubMed: 426281]
- (7). Ostrowski SG, Szakal C, Kozole J, Roddy TP, Xu J, Ewing AG, Winograd N. Anal. Chem 2005;77:6190–6196. [PubMed: 16194078]
- (8). Takats Z, Wiseman JM, Gologan B, Cooks RG. Science 2004;306:471-473. [PubMed: 15486296]
- (9). Wiseman JM, Ifa DR, Song Q, Cooks RG. Angew. Chem., Int. Ed 2006;45:7188-7192.
- (10). Wiseman JM, Ifa DR, Venter A, Cooks RG. Nat. Protoc 2008;3:517–524. [PubMed: 18323820]
- (11). Linton RW, Goldsmith JG. Biol. Cell 1992;74:147–160. [PubMed: 1511242]
- (12). Chehade F, de Labriolle-Vaylet C, Moins N, Moreau MF, Papon J, Labarre P, Galle P, Veyre A, Hindie E. J. Nucl. Med 2005;46:1701–1706. [PubMed: 16204721]
- (13). Clerc J, Fourre C, Fragu P. Cell Biol. Int 1997;21:619–633. [PubMed: 9693832]
- (14). McEwen CN, McKay RG, Larsen BS. Anal. Chem 2005;77:7826–7831. [PubMed: 16316194]
- (15). Kertesz V, Van Berkel GJ. Rapid Commun. Mass Spectrom 2008;22:2639–2644. [PubMed: 18666197]
- (16). Northen TR, Yanes O, Northen MT, Marrinucci D, Uritboonthai W, Apon J, Golledge SL, Nordstrom A, Siuzdak G. Nature 2007;449:1033–1036. [PubMed: 17960240]
- (17). Woo HK, Northen TR, Yanes O, Siuzdak G. Nat. Protoc 2008;3:1341–1349. [PubMed: 18714302]
- (18). Want EJ, Nordstrom A, Morita H, Siuzdak G. J. Proteome Res 2007;6:459–468. [PubMed: 17269703]
- (19). Wilcken B. J. Inherit. Metab. Dis 2007;30:129–133. [PubMed: 17342450]
- (20). Marko-Varga G, Lindberg H, Lofdahl CG, Jonsson P, Hansson L, Dahlback M, Lindquist E, Johansson L, Foster M, Fehniger TE. J. Proteome Res 2005;4:1200–1212. [PubMed: 16083270]
- (21). Fiedler GM, Baumann S, Leichtle A, Oltmann A, Kase J, Thiery J, Ceglarek U. Clin. Chem 2007;53:421–428. [PubMed: 17272489]
- (22). Villanueva J, Philip J, Entenberg D, Chaparro CA, Tanwar MK, Holland EC, Tempst P. Anal. Chem 2004;76:1560–1570. [PubMed: 15018552]
- (23). Pan Z, Gu H, Talaty N, Chen H, Shanaiah N, Hainline BE, Cooks RG, Raftery D. Anal. Bioanal. Chem 2007;387:539–549. [PubMed: 16821030]
- (24). Reyzer ML, Caprioli RM. Curr. Opin. Chem. Biol 2007;11:29–35. [PubMed: 17185024]
- (25). Knochenmuss R. Analyst 2006;131:966–986. [PubMed: 17047796]
- (26). Hsieh Y, Casale R, Fukuda E, Chen J, Knemeyer I, Wingate J, Morrison R, Korfmacher W. Rapid Commun. Mass Spectrom 2006;20:965–972. [PubMed: 16470674]
- (27). Wiseman JM, Ifa DR, Zhu Y, Kissinger CB, Manicke NE, Kissinger PT, Cooks RG. Proc. Natl. Acad. Sci. U.S.A 2008;105:18120–18125. [PubMed: 18697929]
- (28). Naheed M, Green B. Curr. Med. Res. Opin 2001;17:223–229. [PubMed: 11900316]
- (29). The Parkinson Study Group. N. Engl. J. Med 1999;340:757–763. [PubMed: 10072410]
- (30). Tome M, Moreira E, Perez-Figares JM, Jimenez AJ. J. Neural Transm 2007;114:983–994. [PubMed: 17458496]
- (31). Lindon JC, Holmes E, Nicholson JK. FEBS J 2007;274:1140–1151. [PubMed: 17298438]
- (32). Trauger SA, Go EP, Shen Z, Apon JV, Compton BJ, Bouvier ES, Finn MG, Siuzdak G. Anal. Chem 2004;76:4484–4489. [PubMed: 15283591]
- (33). Edwards SR, Minto CF, Mather LE. Br. J. Anaesth 2002;88:94–100. [PubMed: 11881891]

(34). Silwood CJ, Lynch E, Claxson AW, Grootveld MC. J. Dent. Res 2002;81:422–427. [PubMed: 12097436]

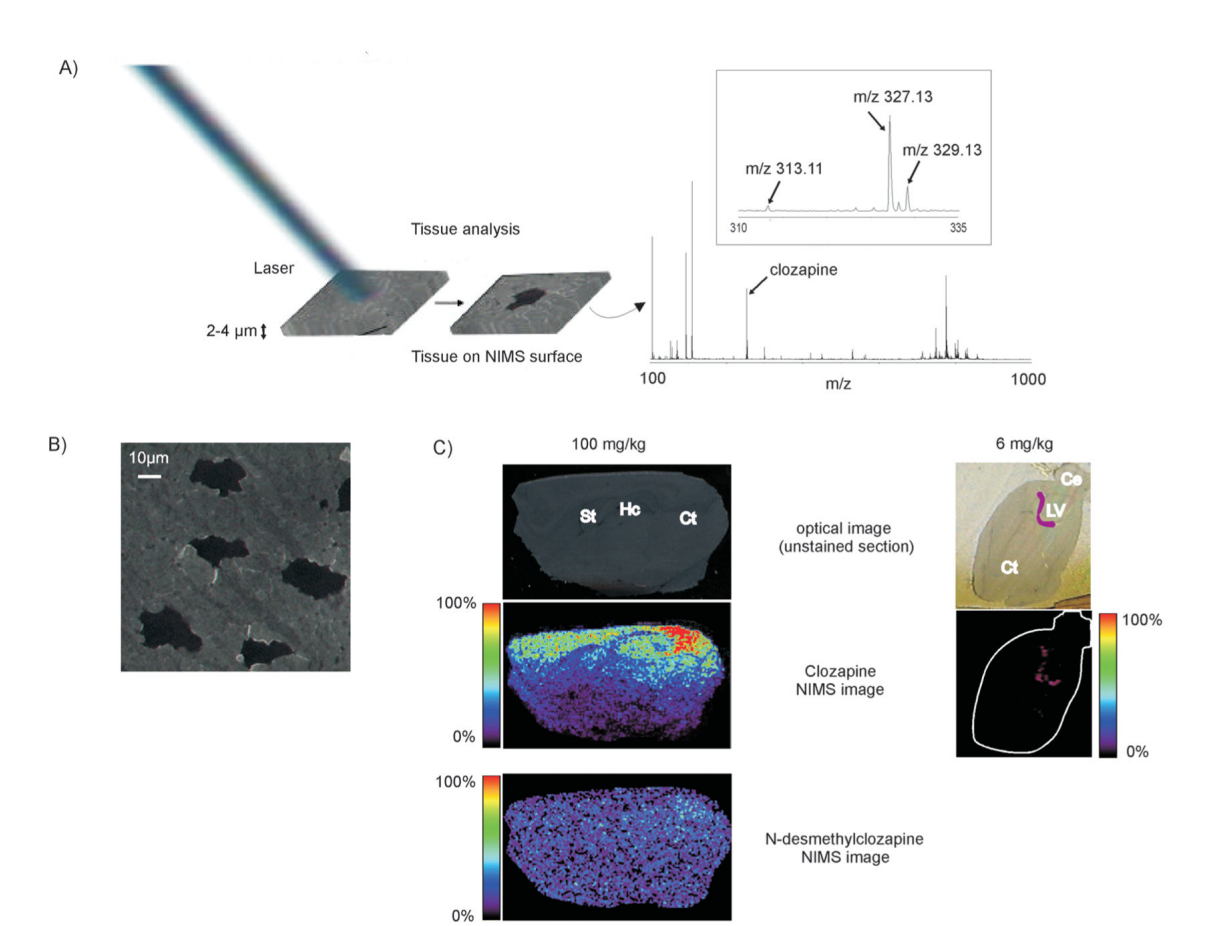
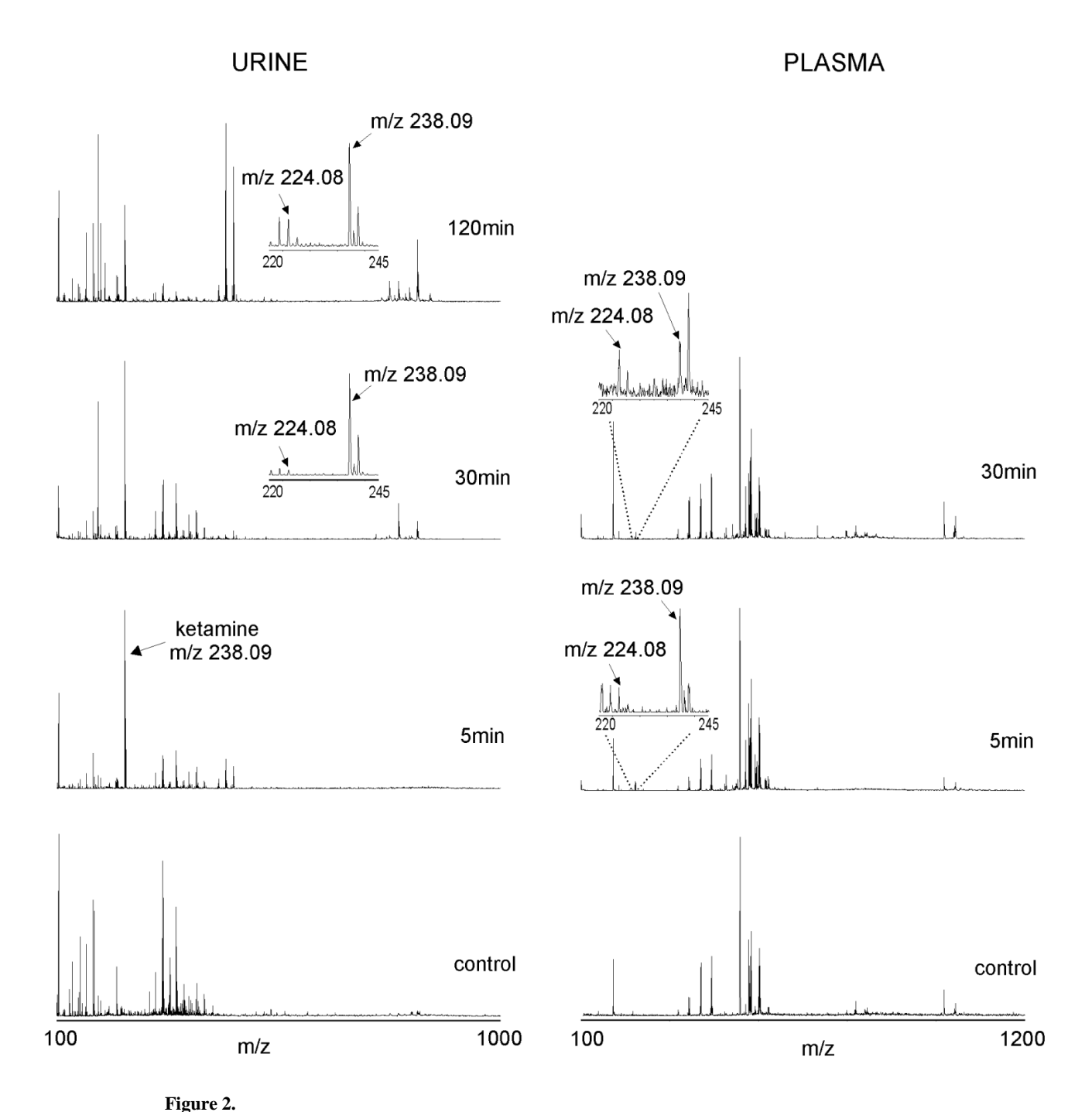
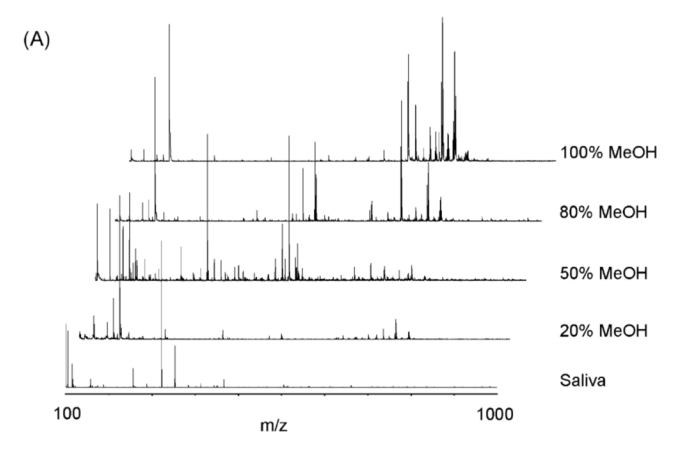


Figure 1. The concept of tissue imaging with laser-NIMS: (A) The tissue slice (2–4  $\mu$ m thick sections) is placed directly on the NIMS surface and is subjected to laser irradiation (~0.1 J/(cm<sup>2</sup> pulse))

is placed directly on the NIMS surface and is subjected to laser irradiation ( $\sim$ 0.1 J/(cm<sup>2</sup> pulse)) resulting in desorption/ionization of endogenous metabolites and xenobiotics. The full-MS mode mass spectrum shows the presence of intact clozapine (m/z 327.13) and N-desmethylclozapine (m/z 313.11) in the brain tissue. Inset shows the isotopic distribution of clozapine characterized by the chloride atom. (B) Nitrogen laser beam irradiation produces 15-20  $\mu$ m diameter "etched" areas (black area). The photograph shows the sagittal unstained section of a mouse brain after MS adquisition on NIMS chip (scale bar: 10  $\mu$ m). (C) Top, unstained sections of brain slices (sagittal) before NIMS analysis. Hc, hippocampus; St, striatum; Ce, cerebellum; LV, lateral ventricle; Ct, cortex. Middle, NIMS clozapine images (dose: 100 mg/kg rat and 6 mg/kg mouse). Bottom, NIMS N-desmethylclozapine image (dose: 100 mg/kg). For easy visualization, the purple mark in the unstained section (6 mg/kg) indicates clozapine localization by NIMS. In the NIMS image, the edge of the tissue has been also highlighted in white.



Direct detection by NIMS of ketamine (m/z 238.09) and its major metabolite norketamine (m/z 224.08) from urine and plasma. Mass spectra of fresh urine and plasma in the 5, 30, and 120 min postdose mouse.



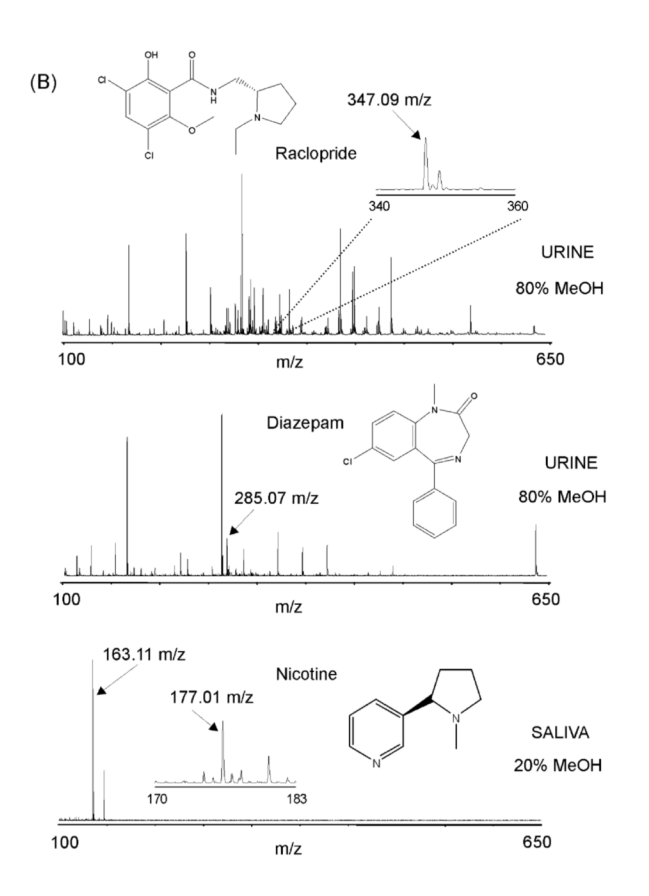


Figure 3. NIMS *in situ* metabolite extraction from saliva and urine. (A) Mass spectra of the direct analysis of human saliva (nonsmoker) (bottom MS) and on-plate extractions using 20%, 50%, 80%, and 100% methanol/water from the original spot. (B) Mass spectra corresponding to 20% methanol/water extraction from deposited saliva on the NIMS chip from an active smoker (bottom MS). Urine containing diazepam at 50 ng/mL and raclopride at 100 ng/mL was deposited on the NIMS chip, and on-plate extraction with 80% methanol/water was analyzed in an adjacent spot observing the presence of these drugs.

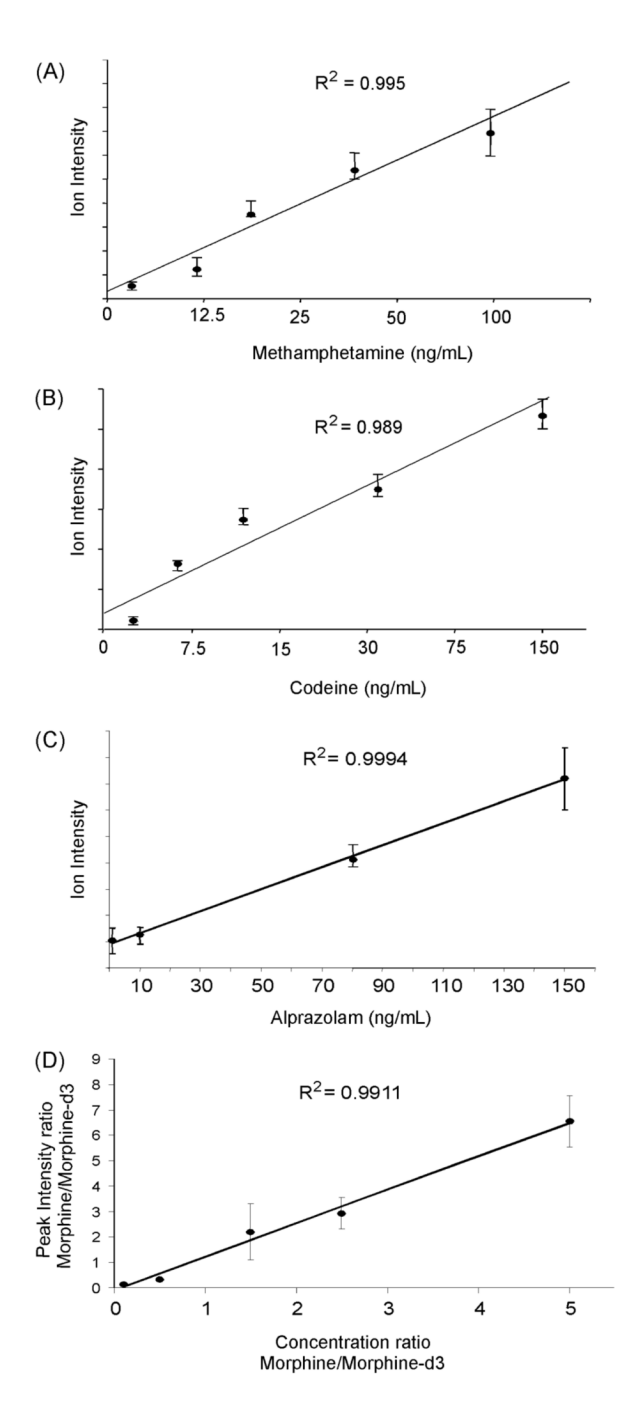


Figure 4. Sensitivity and linear response of NIMS. (A—C) Plots representing the ion intensity response of methamphetamine, codeine, and alpralozam spiked in serum at different concentrations. NIMS shows linear response in the 1–150 ng/mL range, indicating its suitability for quantification analysis. (D) Plot representing the ion intensity response of morphine spiked in serum at different concentrations in the presence of an internal deuterated standard (morphine- $d_3$ ) at 100 ng/mL. The error bars represent the standard deviation.

Table 1

Limit of Detection and Linear Response

compound	LOD for pure compound (amol)	range of linear response in serum (ng/mL)
alprazolam	150	1-150
morphine	850	1-150
methamphetamine	500	1-150
codeine	250	1-150